Doctoral Dissertation

博士論文

Effects of imposed bending on the regulation of oscillatory movement in sea urchin sperm flagella

(ウニ精子鞭毛における振動運動の制御に対する屈曲の効果)

A Dissertation Submitted for the Degree of Doctor of Philosophy

October 2020

令和 2 年 10 月博士（理学）申請

Department of Biological Sciences, Graduate School of Science,
The University of Tokyo

東京大学大学院理学系研究科

生物科学専攻

Yasuhide Izawa

伊澤　寧秀

Acknowledgements

I thank my thesis advisor, Dr. Chikako Shingyoji for giving me thoughtful advice throughout this work. I also thank Professor Winfield S. Sale for discussion and improving of the manuscript. I also thank the director and the staff of the Misaki Marine Biological Station, the University of Tokyo, the Education and Research Center for Marine Biology, Tohoku University, and the Tateyama Marine Laboratory, Ochanomizu University for supplying sea urchins. Lastly, I thank my family for their warm support throughout this study.

Abstract

Cyclical bending of eukaryotic flagella is caused by the orchestrated co-operation of dynein-driven sliding between doublet microtubules within the axoneme. There, oscillation is an essential feature to characterize the molecular mechanisms involved in flagellar movement. In addition to ATP concentration, the mechanical strain of bending in itself contributes to the mechanism of oscillation. I devised a novel experimental system to define the basic factors required for the induction of oscillation. Using such set-up, I examined the effects of mechanical deformation on flagellar responses of demembranated immotile sea urchin sperm flagella held with two glass-microneedles, at very low concentrations of ATP below the threshold required for spontaneous beating. Oscillation-like responses occurred after induction of a pair of planar bends near the glass surface. After induction of paired bends by an application of mechanical deformation at 1.5-2.0 μmol l^{-1} ATP without further glass-microneedle movement, I observed the transition of some paired bends to further stages such as growth and propagation, switching of bend directions, and often even to oscillation-like cyclical bending. In order to achieve cyclical beating, velocities of bend propagation towards the flagellar tip should be kept at a certain level. Synchronous decay of the preceded pair of bends was essential for the constant formation of new bends at the basal region of the flagella. By an analysis of spacio-temporal changes of paired bends, I found that the oscillation-like beating always began with the development of a principal bend (P-bend) at the basal region of the flagellum that follows a preceded reverse-bend (R-bend). Those results clearly indicate that the mechanical strain of bending plays a major role in regulating the

oscillation. Further, constant activity of R-bend is important in the initiation of bends in the flagellar movement.

List of abbreviations

BR: bend formation and relaxation
GP: bend growth and propagation
SW: switching
BEAT: beating

Contents

Chapter 1: Introduction

Eukaryotic flagella and cilia are unique biological apparatuses to develop beating force in the aqueous environment. Both consist of an architecture called "axoneme" or "9+2 structure" i.e. central pair of singlet microtubules surrounded by nine doublet microtubules. A pile of evidences revealed that the bending within cilia and flagella is caused by ATP-driven sliding between doublet microtubules by dynein; the motor protein which is periodically placed along the longitudinal axis of nine doublet microtubules. After pioneering work by Afzelius who demonstrated the presence of 9+2 structure, Satir succeeded to clarify the ultrastructure of beating cilia. He showed that the lengths of nine peripheral fibers (doublets) were kept constant regardless of their position along concave or convex side of bending (Satir, 1968). First experimental evidence of actual sliding was achieved by Gibbons' team (Summers and Gibbons, 1971). Their pioneering work on the reactivation of demembranated cilia and flagella opened a door to the large progress in this field. A new approach with micromanipulation also played another important role to show that the formation of bending in flagella is caused by microtubule sliding. In this work, ATP was locally applied by iontophoresis to the demembranated sea urchin sperm flagellum (Shingyoji, et al., 1977). Brokaw observed the movement of multiple beads attached to the sides of doublet microtubules of demembranated sea urchin sperm flagella. He showed that the beating cycle is associated with sliding, rather than contraction and extension of the doublet microtubules (Brokaw, 1989).

Temporal and spatial control of dynein activity in the axoneme is the basis of flagellar wave formation. It is known that the sliding activity of dynein between doublet microtubules in the 9+2 structure is regulated not only by chemical modulation of the central-pair microtubules and n-drc (nexin-dynein regulatory complex) within the axoneme, but also by the mechanical force by flagellar bending (Hayashibe, et al., 1997;

Ishikawa and Shingyoji, 2007; Morita and Shingyoji, 2004). In the case of sea urchin sperm flagella, a bend started by the sliding at the base of flagellum propagates towards the flagellar tip to produce oscillation, the crucial feature of the flagellar movement. Though the mechanism to switch bending direction is the most important factor to elucidate the oscillation, it is not yet well understood.

Oscillation of the axoneme consists of three stages as follows: 1) formation (or initiation) of a bend at the base of flagellum and its propagation towards the flagellar tip, 2) switching of the bending direction and 3) cyclical repetition of these flagellar responses. Based on the hitherto studies, the mechanism to regulate cyclical bend formation, and switching direction of bending have been extensively discussed in relation to the microtubule sliding within the axoneme. Several hypothetical models were proposed as the mechanism of oscillation. In curvature-controlled model, switching direction of bending at a certain amount of curvature of bend was postulated (Brokaw, 1972, 1982, 1985, 2002). In sliding-controlled model, velocity and amount of microtubule sliding was thought to play key roles for switching (Brokaw, 1975, 1976, 2005; Murase, 1991; Camalet and Julicher, 2000). In geometric clutch model, changes of the distance between doublet microtubules were potential key factors for switching (Lindemann, 1994a,b), while in fluid-structural instability theory, oscillation was involved as one of the intrinsic elastic properties of the entire axial thread (Bayly and Dutcher, 2016).

Many previous studies have shown that external mechanical deformation could affect the regulation of flagellar oscillation. In one study to examine the responses of starfish sperm flagella to mechanical stimulus, further propagation of the bends was blocked when the middle region of the flagellum was touched with a microneedle, but the propagation recovered when the microneedle was detached. It is likely that the

propagation of the bends was hindered because of the delicate deformation of the axoneme, the structure of which is indispensable for initiating active sliding (Okuno and Hiramoto, 1976). In another experiment, they trapped the head of a live sea urchin sperm in the micropipette and vibrated the whole body. They could modulate the frequency of the beat and the sliding velocity by imposed sperm head vibration. Those results suggest that external mechanical stimulation could regulate the activity of dynein in the axoneme (Gibbons, et al., 1987: Shingyoji, et al., 1991b). It was later shown, that the activity of dynein molecules along doublet microtubules in the axoneme could be modulated by externally applied mechanical force and affects the microtubule sliding velocity, as well (Hayashibe, et al., 1997; Morita and Shingyoji, 2004). It was revealed further, that the direction of flagellar bending is switched by the activity of dynein, and that the cooperative control of these dynein activities induced by the mechanical signal of bending is the basis of the oscillatory movement of flagella (Morita and Shingyoji, 2004; Hayashi and Shingyoji, 2008). In addition, imposed sinusoidal vibration to sea urchin sperm head changed the normal oscillation of flagella. The beat frequency and bend amplitude of flagella could be modulated while keeping the stability or regularity of the bending wave (Shingyoji, et al., 1991b, 1995).

To elucidate the controlling mechanism of flagellar oscillation, Ishikawa and Shingyoji (2007) developed a new experimental system in which mechanical perturbations were applied to demembranated, motionless sperm to induce flagellar bending response at low ATP concentration such as 2.0-3.0 μmol l^{-1} (Ishikawa and Shingyoji, 2007). They showed that the mechanical bending imposed to flagellum or a mechanical pulse to a sperm head by tapping manipulator were effective to induce flagellar responses. They also suggested the presence of critical (threshold) ATP

concentration to induce flagellar bending responses around 2.0 μmol l^{-1}. Thus, a capability of external mechanical stimuli to induce oscillation was suggested, even below the threshold levels of ATP (Ishikawa and Shingyoji, 2007).

In this work, I attempted to find the important factors governing flagellar oscillation. Finally, I could define the experimental conditions to induce oscillation movements of immotile sea urchin flagellum under sub-threshold levels of ATP. The results obtained during this work were new and the main parts were published in J. Experimental Biology, vol. 223 (2020), as a Research Article by Dr. Shingyoji and I, entitled "Mechanical induction of oscillatory movement in demembranated, immotile flagella of sea urchin sperm at very low ATP concentrations" (Izawa and Shingyoji, 2020).

Chapter 2: Materials and Methods

Demembranated sperm flagella

Sperm obtained from the sea urchin, *Hemicentrotus pulcherrimus* (A. Agassiz, 1863), were used for experiments. To observe the sperm motility, dry sperm was diluted with 250,000 volumes of Ca^{2+}-free artificial seawater (465 mmol l^{-1} NaCl, 10 mmol l^{-1} KCl, 25 mmol l^{-1} $MgSO_4$, 25 mmol l^{-1} $MgCl_2$, and 2 mmol l^{-1} Tris-HCl; pH 8.0). The quality of sperm motility was examined by counting a swimming rate, which was calculated as a percentage of motile sperm observed in randomly chosen microscopic fields of views. The sperm suspension exceeding 80% in swimming rate was used. The spermatozoa were demembranated by 30 times dilution by adding 1.5 ml of demembranating solution (150 mmol l^{-1} potassium acetate, 2 mmol l^{-1} $MgSO_4$, 10 mmol l^{-1} Tris-HCl, 2 mmol l^{-1} EGTA (ethylene glycol-bis (2-aminoethylether) -N,N,N',N'-tetraacetic acid), 1 mmol l^{-1} dithiothreitol (DTT), and 0.04% (w/v) Triton X-100; pH 8.0) by gentle swirling for 45 seconds at room temperature (20-28°C). The demembranation was stopped by 160 times dilution by adding 4.0 ml of Ca^{2+}-free reactivating solution [150 mmol l^{-1} potassium acetate, 2 mmol l^{-1} $MgSO_4$, 10 mmol l^{-1} Tris-HCl, 2 mmol l^{-1} EGTA, 1 mmol l^{-1} dithiothreitol (DTT), and 2% (w/v) polyethyleneglycol (MW 20,000); pH 8.0] without ATP and kept on ice until use. The demembranated sperm was reactivated by various concentrations of ATP just before the observation of flagellar movement.

Mechanical manipulation

Mechanical deformation was applied to a demembranated flagellum with a glass-microneedle made of a glass rod of 1 mm diameter (G-1000; Narishige, Tokyo, Japan) using a micropipette puller (PP-830; Narishige). The glass-microneedle with the tip coated with 0.1% poly-L-lysine (P-1264; Sigma-Aldrich, U.S.A.) was mounted on a

water-pressure micromanipulator (MHW-103; Narishige) on the stage of an inverted microscope with phase-contrast optics (Axiovert 35; Zeiss, Oberkochen, Germany) with a ×40 objective lens. The head of a demembranated motionless sperm and the distal end of the flagellum were caught with the two glass-microneedles and two kinds of deformation were applied. In the axial deformation, the two needles were pointing towards each other. To bend the flagellum, the head of a sperm was moved towards the distal end of the flagellum to impose bending in the presence of 1.0-2.0 μmol l^{-1} ATP. In the lateral deformation, the head-held needle was placed also at some distance away from the other needle. To bend the flagellum, the head-held needle was moved parallel until it pointed towards the other needle. In either method of deformation, the distance between the two needles decreased to approximately 70-80% of the original distance of flagellar length before deformation. All experiments were carried out at room temperature (20-28°C).

Observation, recording and analysis

Flagellar movements were observed with an inverted microscope equipped with phase-contrast optics, and were recorded with an image-intensified CCD camera (C2400-77; Hamamatsu Photonics, Shizuoka, Japan) and a DVD recorder (DMR-EH73V; Panasonic, Tokyo, Japan). Recorded images were captured with a computer and the movements of flagella were captured by using Image J (version 1.47v; National Institutes of Health, Bethesda, MD, U.S.A.). The traces of the waveforms of flagella were manually plotted every 0.7 μm on the captured flagellar waveform image and those plots were connected smoothly by using software, Bohboh (Baba and Mogami, 1985). The flagellar waveform created by this work is called reconstructed waveform in this study.

To analyze the bending waveforms of flagella, the shear angle curves, showing microtubule sliding as a function of position along the length of a flagellum, were used. The shear angle curves are obtained as a difference in angular orientation between the axis of the sperm head and the locus on the flagellum (Gibbons, 1981; Satir, 1968; Warner and Satir, 1974). The curves of the shear angle correspond to the straight lines of reconstructed waveforms and the straight lines correspond to the curves, respectively. Changes of shear angle between two neighboring sequential lines at a given position along the flagellum represent the sliding velocity (rad s^{-1}) (Brokaw, 1991). Shear curves were taken at 1 s intervals in this study.

Chapter 3: Results

Induction of flagellar oscillation by mechanical deformation of demembranated immotile flagella in the presence of very low ATP

It is well known that demembranated sperm flagella of sea urchins show stable beating at around 35-40 Hz (at 20-28°C) in the presence of 20 μmol l^{-1} ATP. Movement of these reactivated sperm flagella is characterized by cyclical formation of bends at the flagellar base and propagation of each bend towards the flagellar tip (Gibbons and Gibbons, 1972). When the ATP concentration was decreased, beat frequency of reactivated swimming sperm decreased (Table 1), and spontaneously beating sperm were not observed at 1.5 μmol l^{-1} ATP. The threshold ATP concentration for spontaneous beating exists between 1.5 and 2.0 μmol l^{-1} (Ishikawa and Shingyoji, 2007).

In this study, I demonstrated that a certain kind of mechanical deformation by manipulation of both the head and a tip of the sperm is capable of inducing demembranated sperm flagella movements in the presence of 1.5-2.0 μmol l^{-1} ATP. This induction of flagellar response is similar to the results reported by Ishikawa and Shingyoji (2007), but the previous report of the bend formation and propagation was interpreted as a result of passive sliding. Here, the critical advance is that mechanical deformation of the demembranated sperm flagella can induce oscillation-like responses, produced by active microtubule sliding, at very low ATP levels.

Mechanical deformation induced various types of bending or oscillation responses depending on the Mg-ATP^{2-} concentration and the proximity of the sperm flagella to the glass surface. In the presence of 1.0 μmol l^{-1} ATP, a bend (or a single bend) (Fig. 1A) was induced but it did not develop further. Similarly, at 1.0 and 1.2 μmol l^{-1} ATP, paired bends were not induced spontaneously or mechanically. However, at 1.5-2.0 μmol l^{-1} ATP, paired bends were induced and further developed into different types of responses,

including an oscillation-like beating (Figs. 1 and 2). In addition, to induce responses at 1.5-2.0 µmol l^{-1} ATP, the sperm flagellum had to be kept at a certain distance above the glass surface. The distance of the flagellum from the bottom surface influenced the beat frequency and sliding velocity of the flagellum. Interestingly, when the sperm flagellum was held at the middle distance from the surfaces, both beat frequency and sliding velocity showed similar values at both 1.5 and 2.0 µmol l^{-1} ATP (Table 2). These results indicate that in the vicinity of the threshold (1.5-2.0 µmol l^{-1} ATP), small changes in ATP concentration are not an exclusive factor determining conditions of oscillation. It has been demonstrated in fish sperm that such an effect of liquid-solid interface on sperm swimming near the bottom surface is important for the regulation of the flagellar motile performance (Boryshpolets, et al., 2013).

Figure 1 shows typical examples of microneedle manipulation to induce flagellar deformation and the resulting flagellar responses. These responses include: bend relaxation (BR; Fig.1B), bend growth and propagation (GP; Fig.1C), and oscillation-like responses that I call here "beating" (BEAT 1and BEAT 2; Fig.1D, E). Details of these four types of responses will be described below.

When the sperm head-held needle was moved in either a lateral or axial direction relative to the sperm longitudinal axis, mechanical deformation first induced a pair of bends [Fig. 1B-E: four panels of recorded images (left) with their traces (right) in D for lateral and E for axial movement; in B for axial and C for lateral movement, respectively]. When the microneedle movement stopped (red triangles, Fig. 1) some flagella began to show further responses. These responses were depicted by reconstructed, superimposed traces in Fig. 1 B-E at the right-hand side of the recorded images. Characteristic changes occurred in the proximal region of the induced paired bends; in BEAT and GP the

propagation of bends was also observed but growth of bends occurred first. Growing waves gradually moved towards the left direction without changing its form and stopped in GP (Fig. 1C), while in BEAT (Fig. 1D, E), bends developed and propagated, and then the direction of bending alternated relative to the flagellar axis. In BEAT most sperm repeated more than five cycles: a sperm shown in Fig. 1D, 1E continued for 3.5 cycles and least 5 cycles of response, respectively. The response shown in Fig. 1B appears similar to normal beating, but each bend fails to show growth and propagation. Two bends of opposite curvatures showed a slight increase and then decrease in their curvature (Fig. 1B). I call such apparent elastic responses bend relaxation (BR).

Here, I summarize conditions to induce oscillation-like response at 1.5-2.0 μmol l^{-1} ATP. The following three conditions were essential. 1) When I applied mechanical deformation to the flagellum, it was necessary to induce a pair of bends at near the base of the proximal region of a flagellum. 2) For formation of a pair of bends, the microneedle holding the head of the sperm needed to be moved towards the other needle holding the tip of the flagellum. 3) All the manipulation and observation of the flagellar responses needed to be carried out by keeping the flagellar beating plane approximately 10-15 μm above the glass surface, resulting in stable flagellar beating by limiting surface tension.

Characteristics of flagellar responses induced by mechanical deformation

In the presence of 1.5-2.0 μmol l^{-1} ATP, four types of responses were observed when paired bends were induced by mechanical deformation, with no further movement of microneedles (Fig. 2). These include BR (Fig. 1B), indicating that simple bend formation of paired bends does not always show bend relaxation owing to elastic normalization. The other three kinds of flagellar responses are BEAT, switching (SW) and GP. In beating,

bend formation was followed by bend growth and propagation that further developed with alternation on both sides of the flagellar axis and more than three beat cycles. Of the 560 trials, 11.3% showed beating (BEAT). SW is similar to BEAT but the number of alternation cycles was less than three. This SW response was observed in 3.2% of 560 cases; 11 cases (2.0%) showed growth of bends and their propagation, but alternations of bend direction did not occur. I call this response growth and propagation (GP). GP is probably a step leading towards bending with SW and BEAT.

As sea urchin sperm flagellar length is quite constant, most of the sperm used for the study showed a flagellar response in the full length of the flagellum with the distance between two needles close to the whole length of the flagellum (Fig. 1D). In contrast, some flagella responses were localized to a more proximal, short region of the flagellum (Fig. 1E). However, all five kinds of responses were observed regardless of various distance between the two needles. Therefore, the data obtained from flagella with various distances between the two needles were analyzed as a group.

Propulsive force of swimming sperm is generated by flagellar oscillatory movement consisting of axial and lateral components of a sperm head movement relative to its longitudinal axis. Among components involved in the sperm movement a slight rotation also occurs (Cosson, et al., 2003). At the stage of bend initiation this regulation is also important. Microtubule sliding in beating flagella is influenced by the lateral deformation but not by axial deformation (Shingyoji, et al., 1991b). Thus, in this study mechanical deformation was applied using two different directional methods: 1) a sperm head-held needle was moved either axially (axial movement) or 2) laterally (lateral movement). Figure 3 shows a rough survey of the effects of both procedures on the occurrence of four types of responses. In Fig. 3A, all 25 responses were obtained from 25

individual sperm (six red plots for lateral movement and 19 blue plots for axial movement). In Fig. 3B, repetitive measurements were carried out in two sperm by using lateral deformation (red symbols) and axial deformation (blue symbols). Notably, there was little difference between the two types of bend induction for BEAT, SW and GP (Fig. 3A, B). However, the effective speed of axial needle movement seems to be more critical than lateral needle movement for stable responses. Also, there appears to be a minimal speed of the needle movement required for SW and BEAT, while speed of needle movement has little effect on BR induction (Fig. 3C).

Roles of microtubule sliding for the regulation of flagellar responses

Among the various responses, BEAT and SW have in common the induction of oscillatory movement through alternating microtubule sliding. In BEAT and SW, the direction of bending regularly switched to both sides of the axis of the axoneme. However, the number of switching events appeared to have a boundary at three cycles. Therefore, I named responses with less than three beat cycles as SW and responses with more than three cycles as BEAT. To gain a deeper understanding of the role of microtubule sliding in the flagellar response, shear curves in BEAT, SW, GP and BR were obtained and compared (Fig. 4A, C, D-F). (Gibbons, 1981; Satir, 1968; Warner and Satir, 1974).

In BR, once the paired bends were induced, their shear curves showed stable changes during their tip-ward movement of the bend (Fig. 4E), indicating that the wave changes are caused by passive microtubule sliding. In contrast, bend propagation occurring during BEAT, SW, and GP is an active process with characteristic changes in the amplitude of shear curves (Fig. 4A, C, D). More precisely, in GP, the shear angle increased in the early phase of propagation (Fig. 4D) and its largest angle was maintained

in the later phase of propagation. In SW and BEAT, growth of bends in one direction induced an increase in shear angles in the early phase of each cycle (Fig. 4A, and C). This was followed by the change in bend direction during the later phase of bend propagation.

The above results indicate that the mechanisms controlling flagellar responses involved in GP, SW, and BEAT are different from the mechanism controlling BR. To obtain further information about the cyclical components from differences between BEAT and simple growth and propagation (GP and SW), I studied the wave changes at the beginning as well as at stoppage of BEAT.

Conditions determining start and stop of BEAT

In Fig. 5, I summarize typical waveform changes of three types of responses (BEAT, SW and GP) and use BR as for a reference (Fig.5A, C-E). Responses induced by axial or lateral movement were very similar in each type of response. In lateral needle movement I was able to induce stable flagellar deformation resulting in a pair of slightly asymmetrical bends and oriented with a proximal principal bend (P-bend) and a distal reverse bend (R-bend). Interestingly, bend induction did not result in an oppositely oriented pair of bends. In contrast, during axial needle movement various forms of flagellar deformation were observed. However, in this case again I found that stoppage of a head-held needle movement also resulted in P/R bending pairs. Thus, when axial deformation was applied, as well as lateral deformation was applied, new responses started from growth of a P-bend. This type of response, owing to axial deformation, was induced in not only BEAT but also in SW and GP (Fig. 5A, C, D). Flagellar waves appearing at initiation of fish sperm motility show processes similar to those described here (Prokopchuk, 2015).

Propagation velocity determines the regulation of oscillation

To address the conditions regulating the oscillatory response, shear curves (Fig. 4) were carefully examined and the propagating velocities of wave components were compared (Fig. 6). More precisely, for oscillation, I focused on: 1) growth of bends near the flagellar base, 2) propagation of the grown bends that maintain their size, 3) propagation of the bends with slight decrease in size, and 4) switching of directions in the growth and propagation of bends. Bending waves induced in the opposite directions look similar but are slightly different. They are related to P- and R-bends.

When the responses show oscillation ("gain of oscillation"; Fig. 6), the waveforms induced by mechanical deformation undergo alternating cycles of bending. Among the responses showing cyclical switching, there were several examples that showed stoppage of oscillation. When the response showed stoppage during cyclical alternation ("loss of oscillation"; Fig. 6), the switching of bending direction did not occur in the last state, and propagation velocity decreased rapidly, although the size of bends was maintained through propagation. In addition to the last state of BEAT (three cases of stoppage at the fourth cycles) as well as SW (three cases of stoppage at the second cycles), the state of loss of oscillation was similar to the last state of GP (growth and propagation), as well as the response of BR (bend formation and relaxation). As I have shown in green bars in Fig. 6B, there were no significant differences in the propagation velocities among these three different conditions.

As a result of comparison of propagation velocities in each wave component, I found two differences between the conditions necessary for induction of gain of oscillation (Fig. 6B) and those for loss of oscillation (Fig. 6B). Stoppage of cyclical oscillation with limited amount of switching was observed in the 1.5th cycle (N=3) in SW

and the 3.5th cycle (N=3) in BEAT, respectively. These responses at the final cycles were categorized into the loss of oscillation (N/N=6/6). Characteristic responses showing a large decrease in propagation velocity, without maintaining a level of bend growth, were recognized in such final cycles before stoppage (Fig, 6B, green bars). This decrease is similar to the GP. However, in the responses belonging to gain of oscillation, in which bending directions cyclically alternated, the propagation velocity after the growth of bending was kept at a high level. Usual states showing cyclical bending are induced in this group (Fig. 6B). Maintaining sufficient bend propagation velocity, without a decrease in propagation velocity after bend growth, seems to be important for induction of oscillation.

Characteristic changes in curvature of the flagellar movement that support oscillation

Curvature is known as one of the important parameters associated with the regulation of oscillation. However, the role of curvature-control in the regulation of oscillation has been difficult to detect. Figure 7 shows the changes in curvature in the induced bends. When the oscillation continued in Fig. 7A, B (BEAT2 and 3), constant changes with stable ranges in curvature were recognized, suggesting that the induced bends propagate while changing their shape. In contrast, without oscillation in Fig. 7C, D (fourth cycle of BEAT1 and second cycle of SW2) the change in curvature decreased and finally the changes disappeared (red arrows).

When I analyzed the change of curvature during propagation of paired bends, I found interesting characteristics. In Fig. 8, curvatures of induced bends obtained during every second (1/30 frames of recording) were depicted in BEAT3 (Fig. 8A), BEAT1 (Fig.

8B), SW2 (Fig. 8C) and GP3 (Fig. 8D). BEAT3 showed nine cycles of repetition, while BEAT1 showed three cycles of oscillation that were followed by the last phase of stoppage (after t=30 s). In two other cases (Fig. 8C, D), the oscillation stopped in SW2 or did not occur in GP3. As the curvature of paired bends increased (red arrows in Fig. 8), the two consecutive bends in curvature (green boxes in BEAT3, BEAT1, and SW2) (Fig. 8A-C) propagated to the end of the flagellum, and this pair of bends became smaller while balancing each other. By decreasing the size in paired bends in a balanced manner, new paired bends started to develop at the basal region of the flagellum (red arrows in Fig. 8). If this reduction of curvature of the paired bends did not occur (indicated by yellow boxes in BEAT1 (from t=30 s) (Fig. 8B) and in SW2 (from t=11 s) (Fig. 8C), new paired bends may not start to grow at the basal region of the flagellum (blue arrows in Fig. 8A-C and in GP3, Fig. 8D). These curvature fluctuation processes and timing coincided very well with the first, second and third cycles in BEAT3 and BEAT1 (Fig. 8A, B).

Chapter 4: Discussion

The mechanism of flagellar oscillation is a long-lasting enigma that has not been clarified for a long time. Oscillatory movement of eukaryotic flagella consists of five kinds of element, including 1) initiation of a bend near the basal end, 2) repetitive bend formation at any place of the flagellum, 3) growth of bends, 4) alternate formation of bends in both directions (switching of bend direction), and 5) bend propagation from the basal region to the flagellar tip. Usually these elements do not appear independently but they work cooperatively. In sea urchin sperm flagella, not only cyclical bending but also bend propagation occurs in almost one plane (Shingyoji, et al., 1991a). The planarity of beating plane is important to discuss the mechanism of oscillation, because the beat plane is related to the orientation of the two central microtubules of the central pair, thereby the beating plane is important to be considered in the this study.

In order to understand the mechanism that regulates the oscillation of flagella, it is necessary to know the boundary conditions for oscillation. Beat frequency of flagella is determined by the ATP concentration (Brokaw, 1975, 1991; Gibbons and Gibbons, 1972; Shingyoji, et al., 1977; Summers and Gibbons, 1971), but it is also true that the frequency of flagella is influenced by an externally applied mechanical stimulus (Baba and Hiramoto, 1978; Lindemann and Rikmenspoel, 1972; Hayashibe, et al, 1997; Morita and Shingyoji, 2004; Shingyoji, et al., 1991b, 1995). Thus, I should consider both the chemical factors of ATP hydrolysis and the mechanical factors of external mechanical stimulation. In this study, I focused on this features and attempted to induce flagellar oscillation by mechanical factors under suppressing the chemical factors caused by ATP hydrolysis as much as possible. I found the essential experimental conditions are those required for planar oscillation under very low ATP concentration. These are: 1) generating the sliding of microtubules so that a pair of bends are formed, 2) maintaining plane of

flagella at a certain distance from the glass surface, and 3) applying mechanical deformation to induce successively a pair of bends near the base of the flagellum.

To define the conditions required for control of oscillation, I focused on the experimental methods of the study of Ishikawa and Shingyoji in 2007. They succeeded in inducing bend formation and bend propagation-like response by mechanical deformation at very low ATP concentrations (2.0-3.0 μmol l^{-1}). I conducted an experiment using highly diluted immotile demembranated sperm flagella and investigated whether the flagellar response and thus oscillation could be induced below the threshold levels of ATP concentrations in this study. As a result, I succeeded in defining the conditions required for induction of oscillation at 1.5-2.0 μmol l^{-1} ATP.

The flagellar responses that were successfully induced in this study were classified into five types. They are formation of a pair of bends (Paired bends), relaxation of the bends (BR), growth of the bends and their propagation (GP), switching of bending direction for a few cycle (SW) and repetitive cyclical bending for more than three cycles (BEAT). Whenever a pair of bends could be induced by mechanical deformation, it was a combination of these five types. When inducing flagellar oscillations at below the threshold ATP concentrations, it was necessary to induce a pair of bends at the basal part of the flagellum. Next important thing was to maintain a stable bending plane in the case of sea urchin sperm owing to the relatively long flagella length (Hayashi and Shingyoji, 2008; Ishikawa and Shingyoji, 2007).

As a result of inducing a number of flagellar responses, there were both oscillating and non-oscillating responses (as it were, complete and incomplete beat cycles). Both SW and BEAT are oscillating responses, while BR and GP are non-oscillating responses. Among the responses of SW and BEAT, a few cases showed a stoppage of the oscillation.

For example, complete oscillation occurs until the 1st cycle of SW and the 1st to 3rd cycles of BEAT, but the oscillation stops at the 2nd cycle of SW and the 4th cycle of BEAT. I grouped these complete oscillation responses and stopped oscillation responses into “Gain-of-oscillation” and “Loss-of-oscillation”, respectively. Analysis of flagellar responses in the groups Gain-of-oscillation and Loss-of-oscillation in Fig. 6 shows that higher propagation velocities are important for achievement of the oscillation throughout all steps of flagellar movement.

I examined the conditions under which the growth of simple bending changes to periodic oscillation that reciprocates on both sides of the flagellum. I set some parameters, such as glass-microneedle movement that captures the sperm head (distance and duration in Fig. 3), the size of the grown bends (wave amplitude in red numbers in Fig.5), and increasing in sliding velocity of flagella (calculated from shear curves in Fig. 4) and compared them. However, these comparisons did not show any difference in effect on transforming to oscillation. But it turns out that the following three conditions are important for oscillation: 1) R-bend, 2) propagation velocity, and 3) curvature of the distal bends.

It is well known that P-bend and R-bend are periodically formed at the basal region of the flagella of sea urchin sperm (Gibbons and Gibbons, 1980). I found that all the responses belonging to BEAT started from the growth of P-bend. The characteristic of starting with the growth of P-bend was the same for SW and GP. And I also found that in SW and BEAT where the oscillation stop occurred, the stoppage always occurred in the middle of P-bend growth. In addition, I observed only one case, there was a response in which the growth process of R-bend appeared with a delay. This flagellar response was named as “BEAT-like SW”. It is shown in Fig. 5B and Fig. 4B. In this response, although

the P-bend growth at proximal region occurred in the first cycle (during 6 s of the first cycle in Fig. 5B), the propagation velocity of this bend gradually decreased at the distal region of the flagellum (during 10 s of the first cycle in Fig. 5B), giving the appearance of oscillation stoppage. This stoppage is very similar to the one that occurs in GP at the distal region of the flagellum (during 9 s or 12 s of the first cycle in Fig. 5D). After that, the curvature of the distal bend became slightly decrease, and the growth of the R-bend started (during 4 s of the 1st cycle in Fig. 5B). As this R-bend grew, the next new P-bend was born again at the basal region of the flagellum (during 4 s of the second cycle in Fig. 5B) and continued to oscillate for another one and a half cycles. This result suggests that whether the R-bend grows or not is the key to the continuation of oscillation. There is a balance between the propagation velocity of the preceding P-bend and that of the newly grown R-bend, and it is highly possible that the R-bend is involved in controlling this balance.

In sea urchin sperm flagella, ATP concentration is around the millimolar level, then there must be a difference in regulation at the base of flagella from that in this study. However, past studies suggest that oscillation-induced processes are similar for both live sperm and reactivated sperm (Gibbons, 1981; Gibbons and Gibbons, 1980). The proximal region of the flagellum at the onset of oscillation is an important region in the formation and propagation of bending. At the starting transient, the region near the base of the flagellum is important in bend formation and propagation of bends. Capturing the tip of the flagellum with a needle did not seem to affect the induction of oscillation in this study. Therefore, the basic mechanism seems to apply to the initiation of normal flagellar bending. Furthermore, it is necessary to consider how to keep the beating plane of flagella in oscillation. It is known that the bending plane of the flagellum is configured

perpendicular to the plane of central-pair (CP), and the stability of this CP is brought about by the interaction between CP and radial spokes (RS). Such an axoneme structure involving CP/RS stabilizes the switching the bending direction mechanism (Lindemann, 1994a, b; Oda, et al., 2014; Shingyoji, 2018; Lin and Nicastro, 2018).

In a study analyzing the process of cyclical development of live and reactivated spermatozoa of sea urchin (Gibbons, 1981; Gibbons and Gibbons, 1980), the pair of bends starting at the flagellar base was initially small and quickly disappeared without propagation. After that, as such bending formation is repeated several times, the bending becomes larger. Finally, the bends separate from the base and propagate to the tip and this is periodically repeated to become oscillation. In contrast, despite the very low ATP concentration, the waveform induced at the flagellar base is relatively large in this study. These differences at the starting transient between live and reactivated spermatozoa are probably owing to the more effective mechanical strains for sperm. In this study, external strains was applied to both a sperm head and the tip of the flagellum. Then the oscillation was probably controlled by the characteristic activity of the dynein molecules that perform a self-regulating function in response to an external force (Shingyoji, 2018; Shingyoji, et.al., 2015; Yoke and Shingyoji, 2017).

The possible effects on the function of the sperm head to generate flagellar oscillation will be discussed. It seems possible to obtain similar results using flagella with the sperm head removed, but it is not easy to capture both the head side and tip side of the flagellum with a glass-microneedle. Previous studies have attempted to induce the flagellar responses after holding the sperm head and the vicinity of the flagellar base together with the same glass-microneedle to prevent the interaction between the head and the flagellar base from moving (Ishikawa and Shingyoji, 2007). The results revealed that

the head-flagellum junction did not play a special role in inducing oscillation. As long as the area of flagella capable of inducing bending was secured, it was possible to induce various flagellar responses by mechanical deformation. However, as the length of the flexible flagellar region decreases, the induction rate of the flagellar responses decreases. Therefore, it can be said that the control of dynein activity by an external force is a basic element in inducing oscillation.

However, it remains a mystery how asymmetry occurs in a pair of bends owing to P-bend and R-bend. The mechanism of R-bend that prevents it from changing due to external influences may play a central role in regulating oscillation (Eshel, et al., 1991, 1992). Since this asymmetry is affected by Ca^{2+}, changes in asymmetry at various Ca^{2+} levels can be an effective way for elucidating the role of R-bend in inducing oscillation.

Conclusion

The aim of this study is to clarify essential factors determining the induction of cyclical beating in flagella. In order to better understand the mechanism of oscillation in the flagellar beating, I devised a unique experimental approach to separate the control of microtubule sliding by mechanical strain from the control of ATP-dependent microtubule sliding. When mechanical deformation of demembranated flagella successfully induced a pair of bends at very low ATP concentrations below that needed for their spontaneous beating, the bends showed various responses as follows. They were, growth and propagation of bends, an alternation of bending direction, and repetition of cyclical bending. Very often, the attenuation of the propagation velocity occurred near the tip of the flagella. These series of responses were orderly regulated by deformation of preceding bends. Though the precise mechanism to determine asymmetrical characteristics of P-bend and R-bend of paired bends is still a mystery, it is highly likely that each bend has a different role in the initiation process of cyclical bending. Whenever a new bend was induced at the base of the flagellum, it started with the growth of P-bend and the stoppage of beating also occurred in the growth process of P-bend, and paired bends with a preceded R-bend did always occur. The presence of preceded R-bend could be an important factor in controlling the continuation and stoppage of oscillation.

This study strongly suggests that ATP-driven microtubule sliding by dynein molecules is controlled, in part, by the strain to produce a pair of bends near the base of the flagellum. The induced pair of bends propagated towards the tip of the flagellum with an increased velocity, while reducing the amount of sliding in the distal region. This process leads to generate a new bend at the basal region of the flagellum. These are the

first experimental demonstrations that defines the basic molecular mechanisms of oscillation underlying flagellar beating.

Table 1. Beat frequency and sliding velocity of spontaneously swimming *Hemicentrortus pulcherrimus* sperm at ATP concentrations above the threshold.

ATP (μmol l^{-1})	Beat frequency (Hz)	Sliding velocity (rad s^{-1})	*N*
1.5	No swimming sperm		
2.0	0.21±0.01	1.09±0.07	16
3.0	0.39±0.08	1.48±0.17	10
5.0	0.51±0.17	2.35±0.77	11

Values are means±s.d.; *N* is the number of cycles counted during stable beating in sperm.

Table 2. Effects of distance from the bottom surface on the beat frequency and sliding velocity of sperm flagella showing beating by mechanical deformation at low ATP levels.

	Distance from the bottom surface under mechanical deformation								
	upper level (> 15 μm)			middle level (5-15 μm)			lower level (< 5 μm)		
ATP (μmol l^{-1})	Beat frequency (Hz)	Sliding velocity (rad s^{-1})	*N*	Beat frequency (Hz)	Sliding velocity (rad s^{-1})	*N*	Beat frequency (Hz)	Sliding velocity (rad s^{-1})	*N*
1.5	n.d.	n.d.		0.14±0.02	1.09±0.16	27	0.03±0.01	0.61±0.07	9
2.0	0.23±0.01	1.16±0.07	16	0.15±0.03	1.01±0.12	35	0.05±0.01	0.80±0.07	6

Values are means±s.d.; upper, middle, and lower level indicates the distance from the glass surface of the flagella; *N* is the number of trials. All responses belonged to the "BEAT" that showed more than three cycles of beating. n.d., not detected.

Fig.1

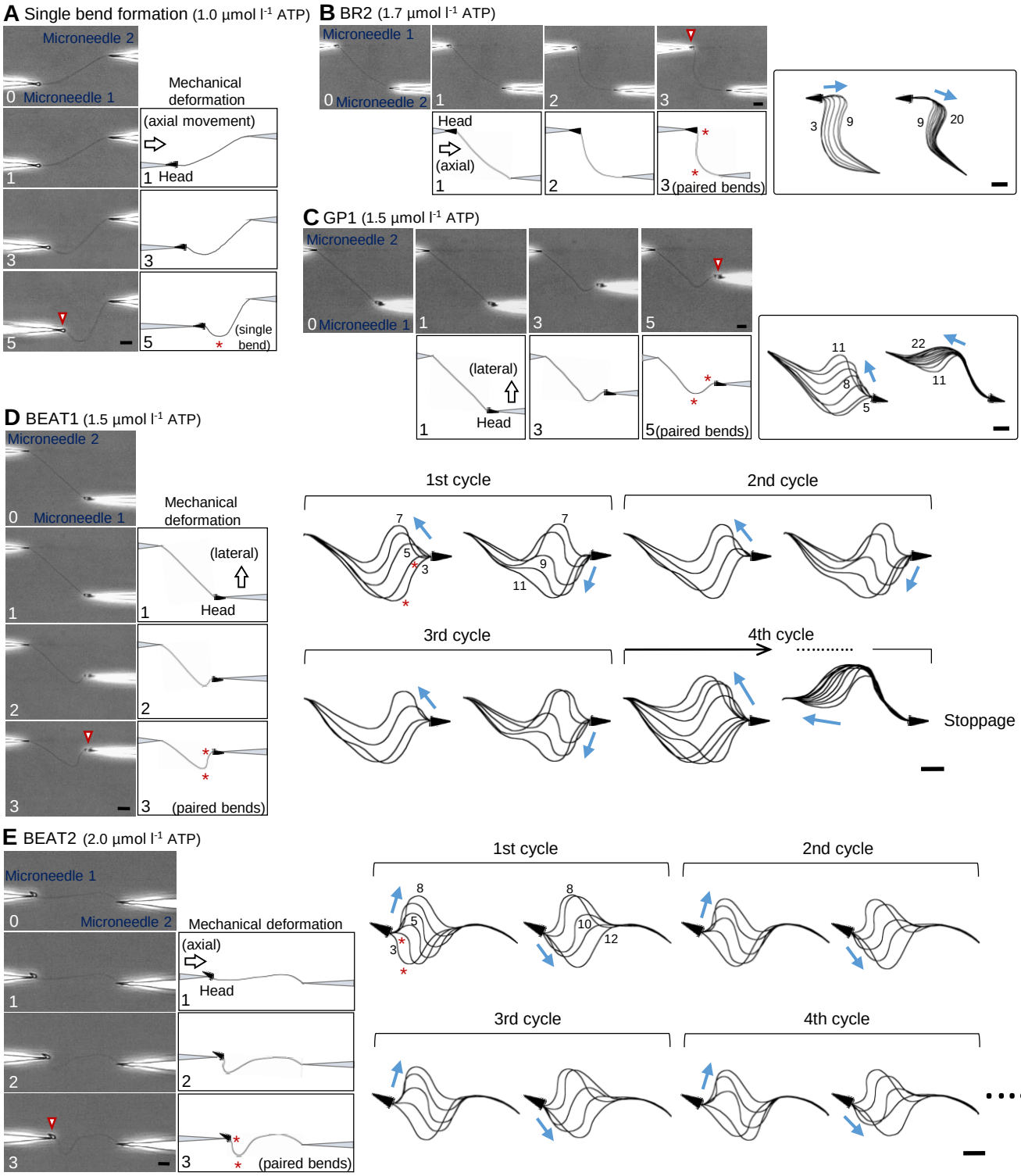
A Single bend formation (1.0 μmol l-1 ATP)
Microneedle 2
0 Microneedle 1
Mechanical deformation
(axial movement)
1 Head
(single bend)
B BR2 (1.7 μmol l-1 ATP)
Microneedle 1
0 Microneedle 2
Head
(axial)
(paired bends)
C GP1 (1.5 μmol l-1 ATP)
Microneedle 2
0 Microneedle 1
(lateral)
Head
(paired bends)
D BEAT1 (1.5 μmol l-1 ATP)
Microneedle 2
0 Microneedle 1
Mechanical deformation
(lateral)
Head
(paired bends)
1st cycle
2nd cycle
3rd cycle
4th cycle
Stoppage
E BEAT2 (2.0 μmol l-1 ATP)
Microneedle 1
0 Microneedle 2
Mechanical deformation
(axial)
Head
(paired bends)
1st cycle
2nd cycle
3rd cycle
4th cycle

Fig. 1.

Sequential images of *Hemicentrotus pulcherrimus* flagellar responses obtained from the DVD recordings. Included are traces at the beginning step of bend induction (A-E) and reconstructed superimposed traces of the flagellar response (B-E): single bend formation (A), bend relaxation (B), bend growth and propagation (C) and beating (D, E). Mechanical deformation was applied to immotile demembranated sperm flagella at (A) 1.0 μmol l^{-1} and (B-E) 1.5-2.0 μmol l^{-1} ATP. Each sperm was caught with two glass-microneedles: microneedles 1 and 2 are holding a sperm head and a flagellar distal region, respectively. Mechanical deformation was applied to the flagellum by moving microneedle 1 towards microneedle 2 by their axial (A, B, E) or a lateral (C, D) movement while maintaining parallel orientation of the two microneedles. Numbers in the lower left corner of panels indicate the time in seconds after the beginning of microneedle movement. Movement of microneedles and changes of flagellar shape during mechanical deformation are also shown in the right-hand traces (1-5 s): a single bend in A and a pair of bends (asterisks) in B, C, D and E were induced. Following stoppage of microneedle 1 (red triangle) and induction of paired bends, four types of responses were observed. They are oscillation-like response (BEAT in D, E), bend relaxation (BR in B) and bend growth and propagation (GP in C). D shows the first to third cycles and the final fourth, incomplete cycle with gradual stoppage. E shows sequential wave changes for four cycles of at least a five-cycle response. Superimposed images in B, C, D and E are reconstructed from recorded images. Scale bars, 10 μm.

Fig.2

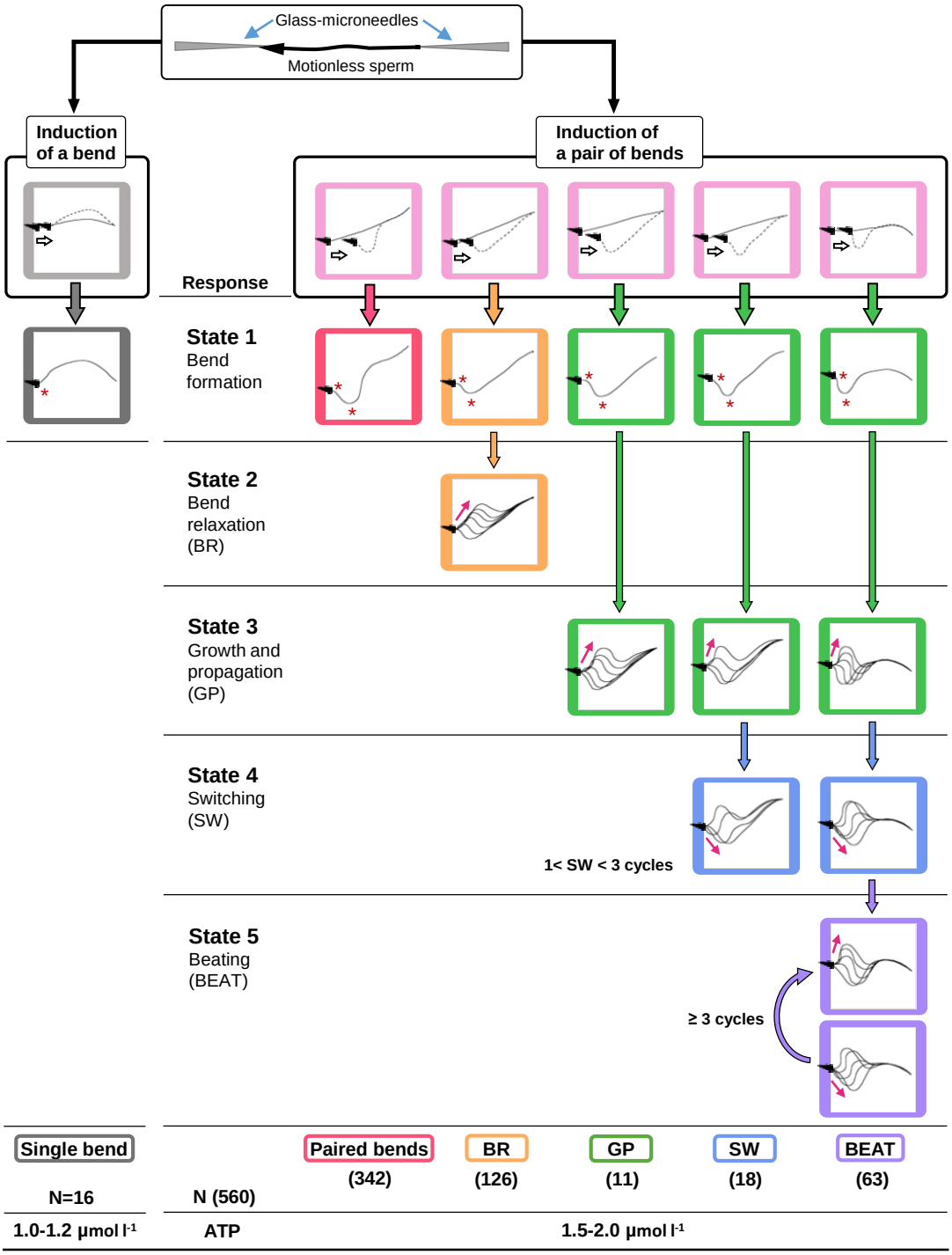
Glass-microneedles
Motionless sperm
Induction of a bend
Induction of a pair of bends
Response
State 1
Bend formation
State 2
Bend relaxation (BR)
State 3
Growth and propagation (GP)
State 4
Switching (SW)
1< SW < 3 cycles
State 5
Beating (BEAT)
≥ 3 cycles
Single bend
N=16
1.0-1.2 µmol l-1
N (560)
ATP
Paired bends (342)
BR (126)
GP (11)
SW (18)
BEAT (63)
1.5-2.0 µmol l-1

Fig. 2.

Schematic diagram summarizing characteristics of flagellar responses induced by mechanical deformation at very low ATP concentrations. At 1.0 and 1.2 μmol l^{-1} ATP, a single bend was induced while a pair of bends was not induced (*N*=16). In contrast, at 1.5-2.0 μmol l^{-1} ATP, mechanical deformation brought about induction of paired bends, which were followed by further flagellar responses (total number of trials = 560 by 127 sperm). All illustrations show typical flagellar waveforms depicted from the recorded images. White arrows in the first row indicate direction of head movement to induce bending by mechanical deformation (grey frames at 1.0-1.2 μmol l^{-1} ATP; pink frames at 1.5-2.0 μmol l^{-1} ATP). In the second row (State 1), red asterisks in the colored frames indicate the bent region of induced paired bends. Following induction of paired bends, further changes were observed and are shown in States 2-5. Of the total 560 cases that showed paired bends, at first bending, no further responses were observed in 342 cases and named paired bends. The first response accompanying the bend formation was bend relaxation (BR; *N*=126). State 2 seems to be independent of States 3-5. State 3 involves growth and propagation (GP) of bends, which appeared in 11 cases out of 560. States 4 and 5 belong to an oscillation-like response with switching direction of bending [SW: a few cycle (<3); BEAT, ≥3 cycles]. Switching (SW) and beating (BEAT) were observed in 18 and 63 cases out of 560, respectively. *N* is the number of induced responses.

Fig.3

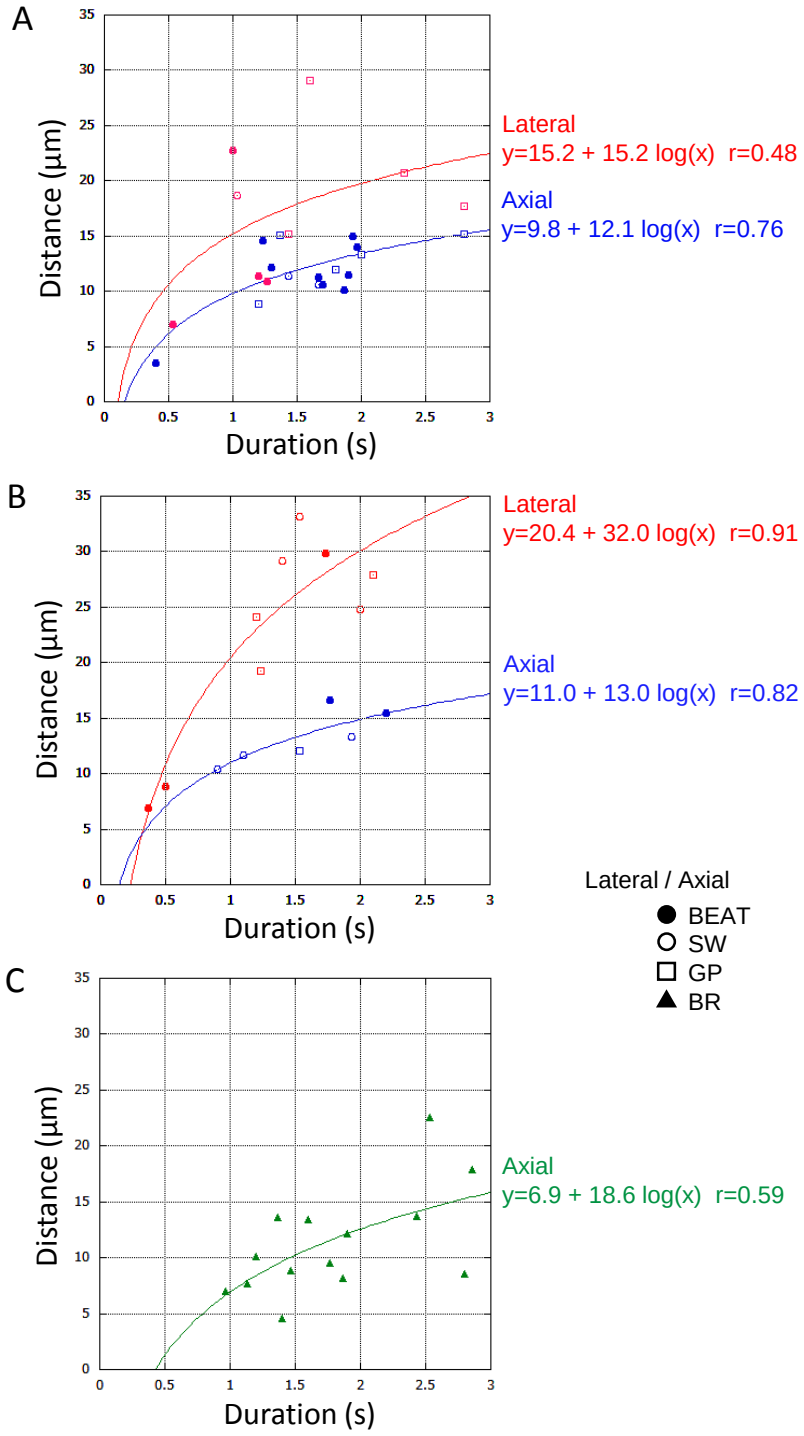
A
Distance (μm)
Duration (s)
Lateral
y=15.2 + 15.2 log(x) r=0.48
Axial
y=9.8 + 12.1 log(x) r=0.76
B
Distance (μm)
Duration (s)
Lateral
y=20.4 + 32.0 log(x) r=0.91
Axial
y=11.0 + 13.0 log(x) r=0.82
Lateral / Axial
BEAT
SW
GP
BR
C
Distance (μm)
Duration (s)
Axial
y=6.9 + 18.6 log(x) r=0.59

Fig. 3.

Effects of the movement of the sperm head-held needle on the induction of flagellar responses. Microneedles holding sperm heads were moved axially or laterally to induce a pair of bends in demembranated flagella at 1.5-2.0 μmol l^{-1} ATP. Distance and duration of the microneedle movement are slightly related to appearance of BEAT, SW and GP (A, B) but not to BR (C) in both axial (blue or green) and lateral (red) needle movements. Twenty-five individual sperm (A), two sperm (B) and 14 sperm (C) were used.

Fig.4

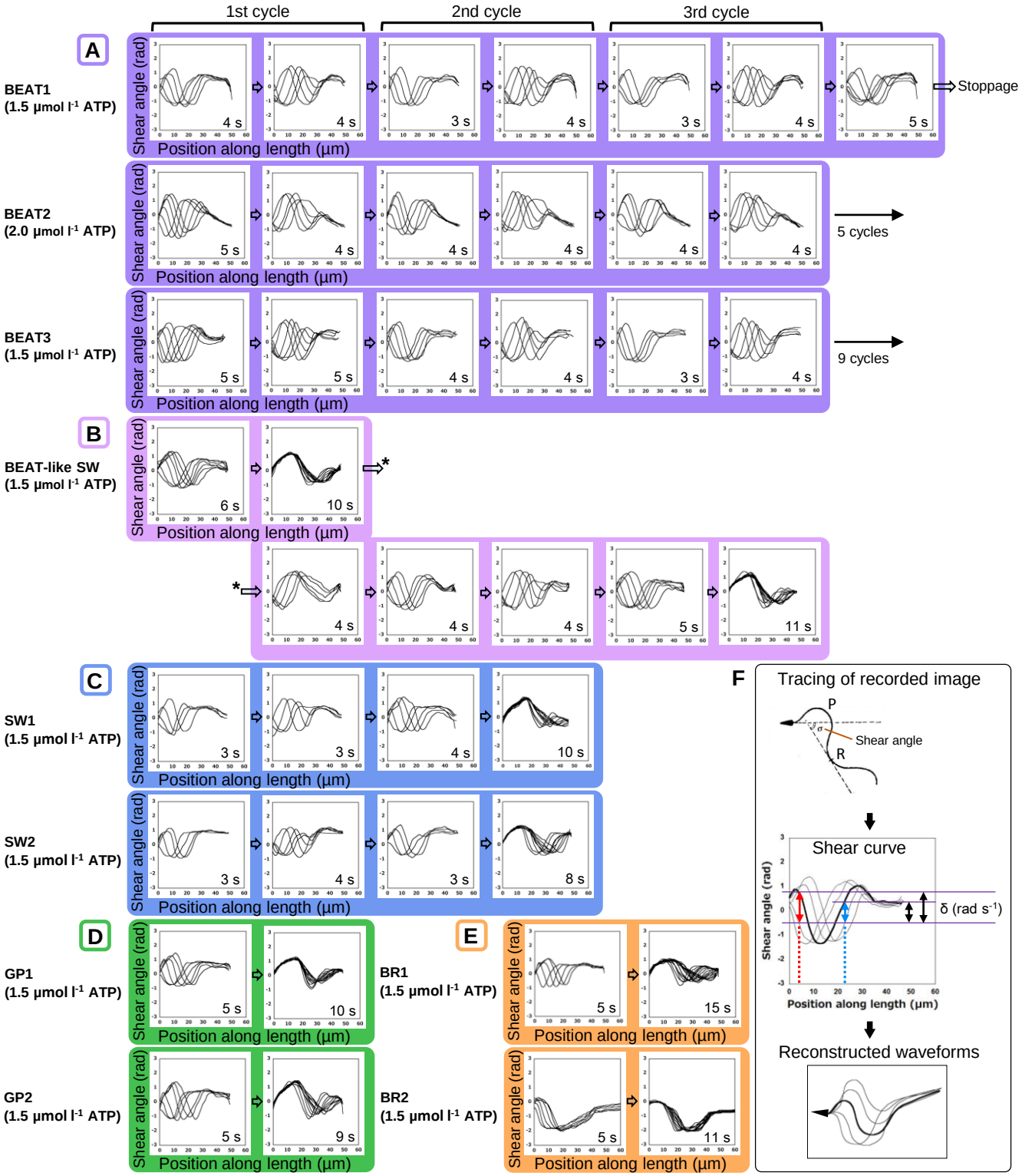
1st cycle
2nd cycle
3rd cycle
A
BEAT1
(1.5 μmol l-1 ATP)
Shear angle (rad)
Position along length (μm)
4 s
4 s
3 s
4 s
3 s
4 s
5 s
Stoppage
BEAT2
(2.0 μmol l-1 ATP)
5 s
4 s
4 s
4 s
4 s
4 s
5 cycles
BEAT3
(1.5 μmol l-1 ATP)
5 s
5 s
4 s
4 s
3 s
4 s
9 cycles
B
BEAT-like SW
(1.5 μmol l-1 ATP)
6 s
10 s
*
*
4 s
4 s
4 s
5 s
11 s
C
SW1
(1.5 μmol l-1 ATP)
3 s
3 s
4 s
10 s
SW2
(1.5 μmol l-1 ATP)
3 s
4 s
3 s
8 s
D
GP1
(1.5 μmol l-1 ATP)
5 s
10 s
GP2
(1.5 μmol l-1 ATP)
5 s
9 s
E
BR1
(1.5 μmol l-1 ATP)
5 s
15 s
BR2
(1.5 μmol l-1 ATP)
5 s
11 s
F
Tracing of recorded image
P
Shear angle
R
Shear curve
δ (rad s-1)
Reconstructed waveforms

Fig. 4.

Typical examples of shear curves showing time-dependent changes of shear angles along the length of the flagellum in five types of responses. Sequential wave changes of each cycle are divided into two panels, and in each panel early phase and a later phase of the response are depicted. (A) Three sequential cycles for BEAT; (C) two sequential cycles for SW; (D) GP; (E) BR. (B) BEAT-like SW: this rare response began with a GP-like response, but after a short pause, a new bend appeared at the flagellar base in opposite bending direction. Such switching of bending direction occurred for two cycles. (F) Procedure to obtain shear curves from measurement of shear angle (top) and reconstructed waveforms based on the shear curves. Changes of shear angle between two neighboring sequential lines at a given position along the flagellum represent the sliding velocity (rad s^{-1}). Shear angles are taken at 1 s intervals. P, principal bend; R, reverse bend; δ, sliding velocity.

Fig.5

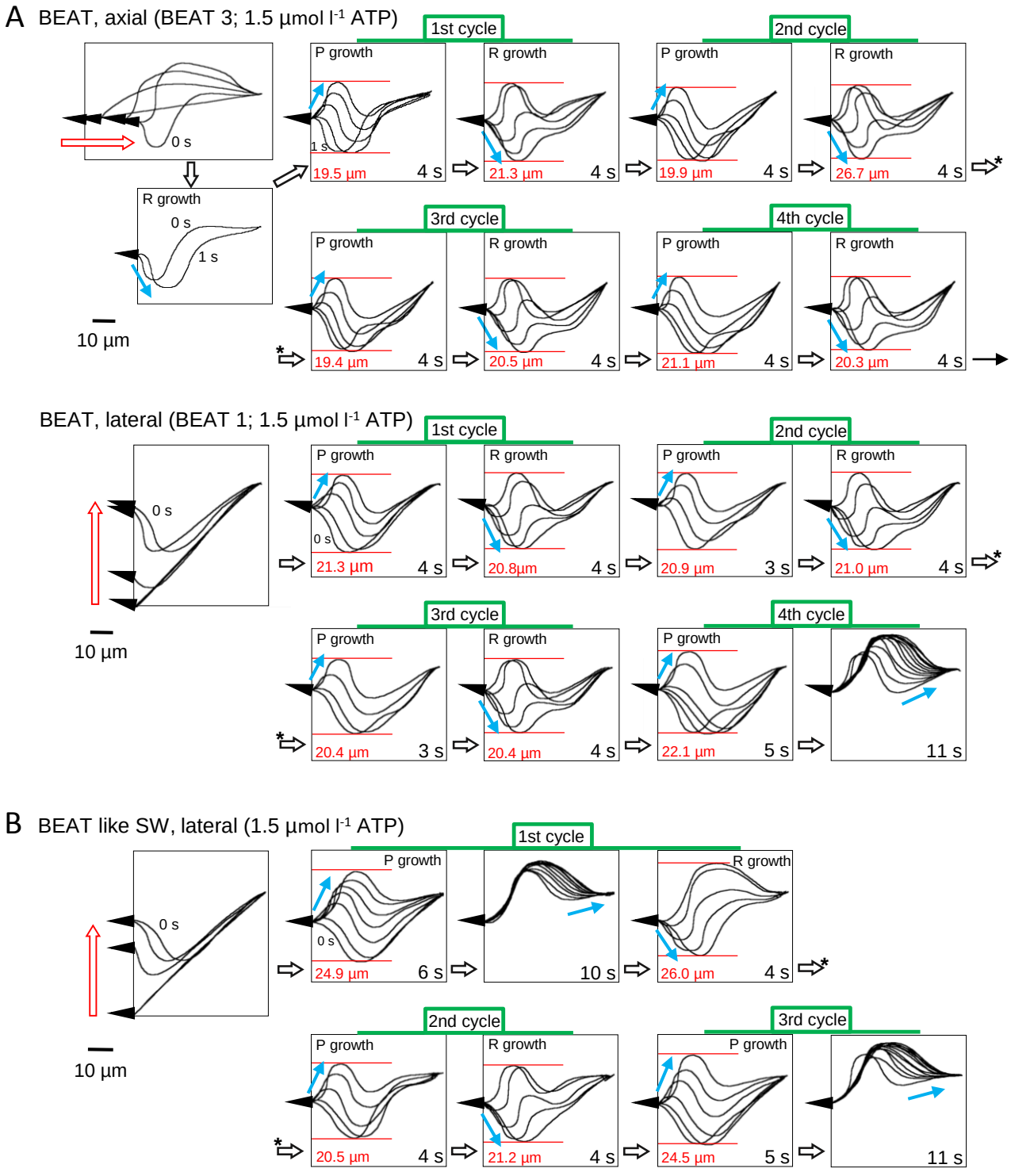
A BEAT, axial (BEAT 3; 1.5 µmol l-1 ATP)
1st cycle
2nd cycle
3rd cycle
4th cycle
P growth
R growth
0 s
1 s
19.5 µm
4 s
21.3 µm
19.9 µm
26.7 µm
19.4 µm
20.5 µm
21.1 µm
20.3 µm
10 µm
BEAT, lateral (BEAT 1; 1.5 µmol l-1 ATP)
21.3 µm
20.8µm
20.9 µm
3 s
21.0 µm
20.4 µm
22.1 µm
5 s
11 s
B BEAT like SW, lateral (1.5 µmol l-1 ATP)
24.9 µm
6 s
10 s
26.0 µm
20.5 µm
21.2 µm
24.5 µm

C SW, axial (SW 1; 1.5 µmol l^{-1} ATP)

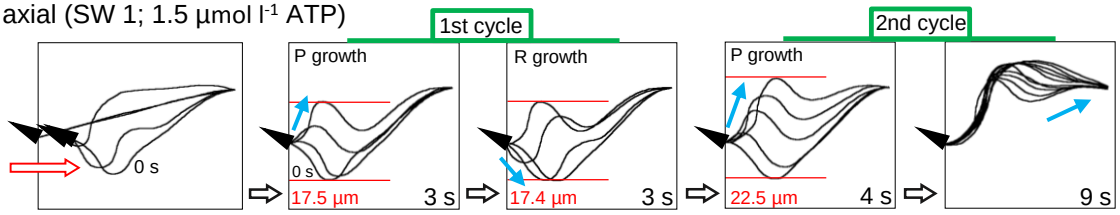

10 µm

SW, lateral (SW 2; 1.5 µmol l^{-1} ATP)

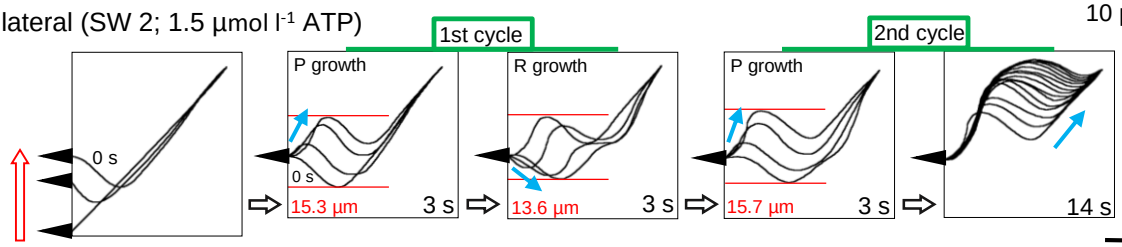

10 µm

D GP, axial (GP 2; 1.5 µmol l^{-1} ATP)

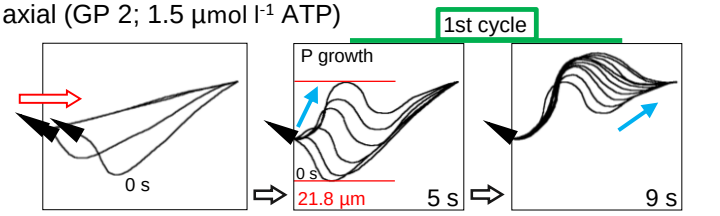

10 µm

GP, lateral (GP 1; 1.5 µmol l^{-1} ATP)

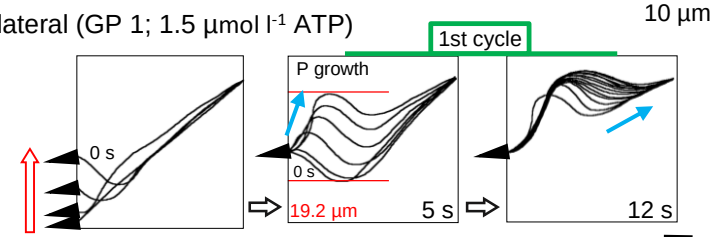

10 µm

E BR, axial (BR 1; 1.5 µmol l^{-1} ATP)

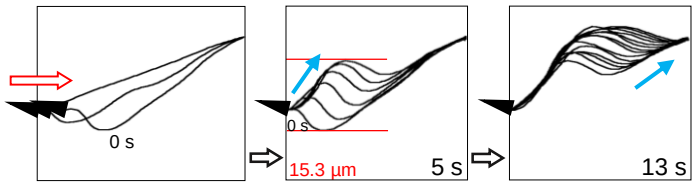

10 µm

BR, axial (BR 2; 1.7 µmol l^{-1} ATP)

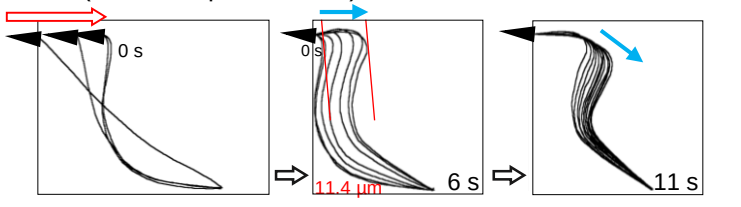

10 µm

Fig. 5.

Typical axially and laterally induced waveform changes for the five types of flagellar responses. The effects of two types of needle movement (axial and lateral) on the waveform changes in five types of responses (A-E) are shown. Sequential wave changes of each cycle are divided into two panels (except in B: two and three panels), including an early phase and a later phase of the response. (A) BEAT; (B) BEAT-like SW; (C) SW; (D) GP; (E) BR. Responses in each type are very similar regardless of the different needle movement. In lateral and axial conditions, a pair of proximal principal bends with a distal reverse bend (P/R bends) is induced at the flagella base (A-D). An exceptional observation was BEAT-like SW (B). Stoppage of beating also occurred at the stage of P-bend propagation (A-D). A detailed explanation of BEAT-like SW (B) is given in the Discussion.

Fig.6

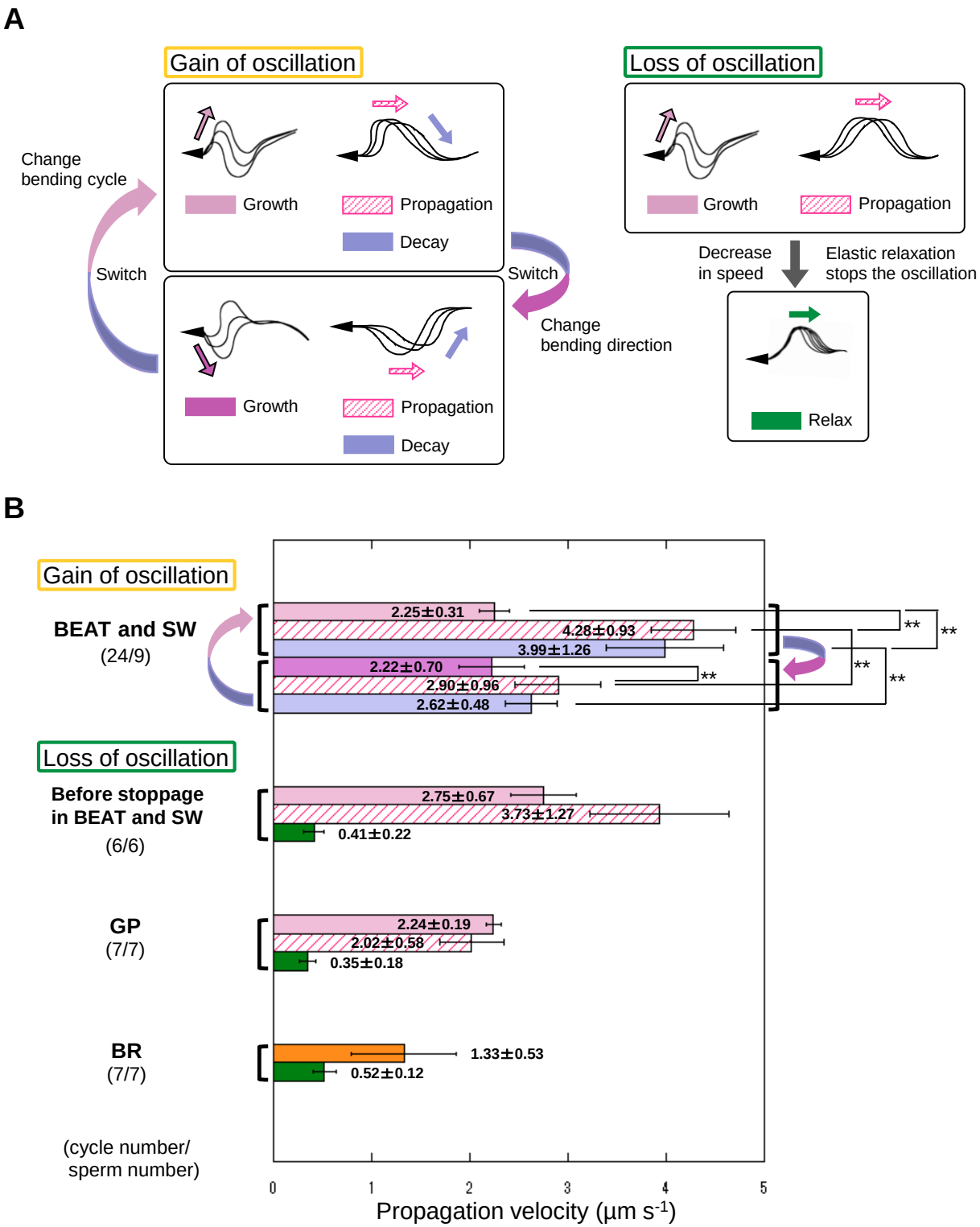
A
Gain of oscillation
Loss of oscillation
Change
bending cycle
Growth
Propagation
Decay
Switch
Switch
Change
bending direction
Growth
Propagation
Decay
Decrease
in speed
Elastic relaxation
stops the oscillation
Relax
B
Gain of oscillation
BEAT and SW
(24/9)
2.25±0.31
4.28±0.93
3.99±1.26
2.22±0.70
2.90±0.96
2.62±0.48
**
**
**
**
**
Loss of oscillation
Before stoppage
in BEAT and SW
(6/6)
2.75±0.67
3.73±1.27
0.41±0.22
GP
(7/7)
2.24±0.19
2.02±0.58
0.35±0.18
BR
(7/7)
1.33±0.53
0.52±0.12
(cycle number/
sperm number)
0
1
2
3
4
5
Propagation velocity (μm s-1)

Fig. 6.

Factors important for the oscillation: mean propagation velocities determine the response, and minimal propagation velocity is required for oscillation. (A) A model for conditions triggering the mechanism of oscillation. Propagation velocity of each wave components was obtained and compared. Factors I focused on as important for oscillation were as follows: 1) growing state of induced bends near the flagellar base, 2) propagation of the grown bends while maintaining their size, 3) further propagation of the bends with slight decrease in size, and 4) switching of directions in the growth and propagation of bends. For oscillatory beating (gain of oscillation) these states (states 1-3) appeared regardless of the direction of a newly grown bend. Propagation velocities on one side and those on the opposite side were alternately observed. These responses were categorized into a gain of oscillation group. The loss of oscillation group, not accompanied by oscillation (such as in GP and BR), showed propagation of induced bends on only one side. Pink, hatched and purple bars indicate propagation velocities of states 1, 2 and 3, respectively. (B) Relationship between oscillatory conditions and wave propagation velocities. Green and orange bars show velocities of bend movement, observed just before stoppage of movement and BR, and belonging to a loss of oscillation group. Of all the flagellar responses, SW and BEAT showed oscillation-like cyclical bending, while some cases of SW and BEAT showed stoppage after only a few cycles of bending. Responses during continuous repetition of cyclical bending were categorized as gain of oscillation, and responses during cyclical bending before stoppage were categorized as loss of oscillation. Means ± s. d. of propagation velocity are shown. Numbers in parentheses (*N*/*N*) indicate the number of cycles analyzed (first digit) obtained from the number of sperm (second digit). Asterisks indicate that the differences are statistically significant

(Mann-Whitney U test; **P<0.01).

Fig.7

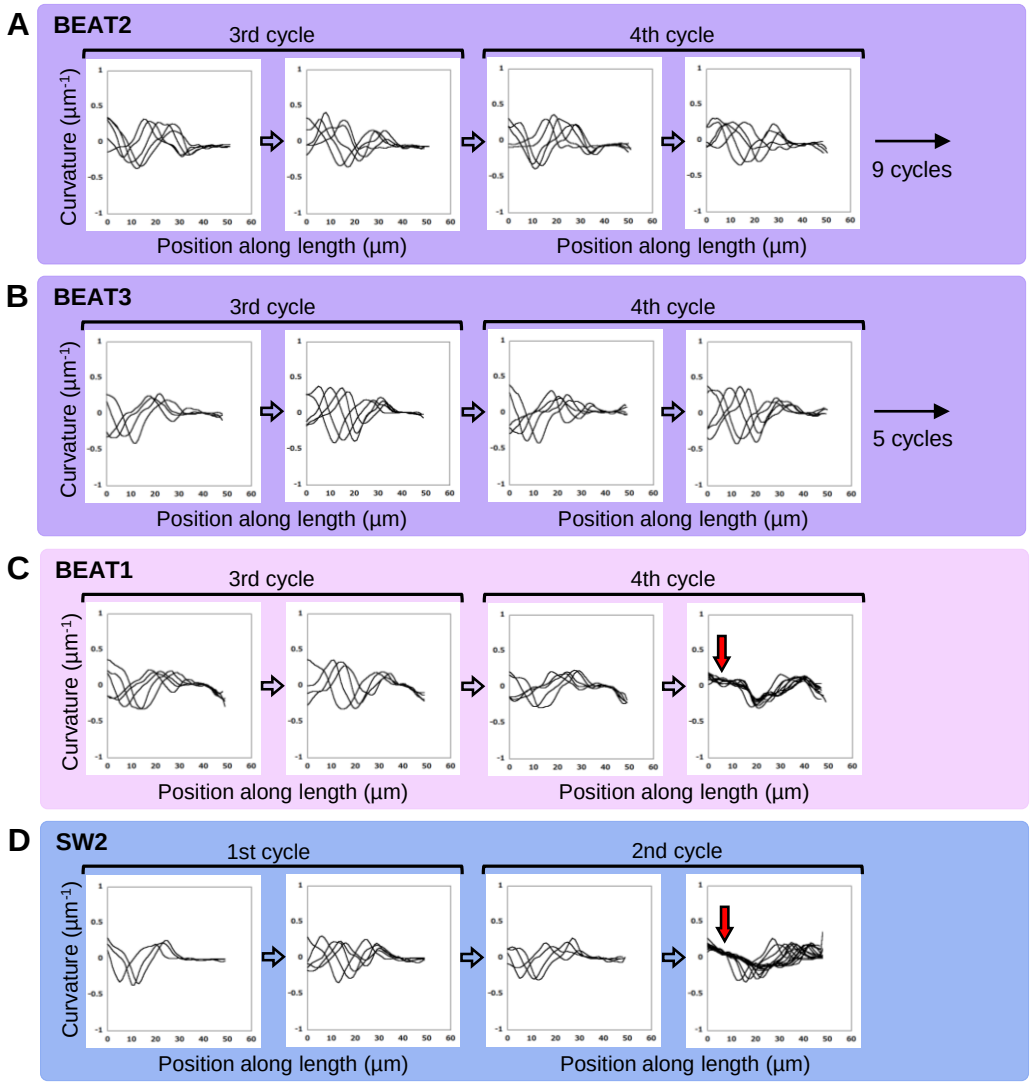
A
BEAT2
3rd cycle
4th cycle
Curvature (μm-1)
9 cycles
Position along length (μm)
Position along length (μm)
B
BEAT3
3rd cycle
4th cycle
Curvature (μm-1)
5 cycles
Position along length (μm)
Position along length (μm)
C
BEAT1
3rd cycle
4th cycle
Curvature (μm-1)
Position along length (μm)
Position along length (μm)
D
SW2
1st cycle
2nd cycle
Curvature (μm-1)
Position along length (μm)
Position along length (μm)

Fig. 7.

Changes of curvature along flagellar length in BEAT and SW responses. BEAT2 (A), BEAT3 (B) and BEAT1 (C) are the same sperm flagella shown in Fig. 4A. SW2 (D) is obtained from the data used in Fig. 4C showing 1.5 cycles of beating. Different from the regular repetition of curvature changes in each cycle (in A and B), in C and D, just before the stoppage of beating, curvature changes disappeared (red arrows in the last panel). Curvatures were calculated every second for the recorded images (at 30 frames s^{-1}).

Fig.8

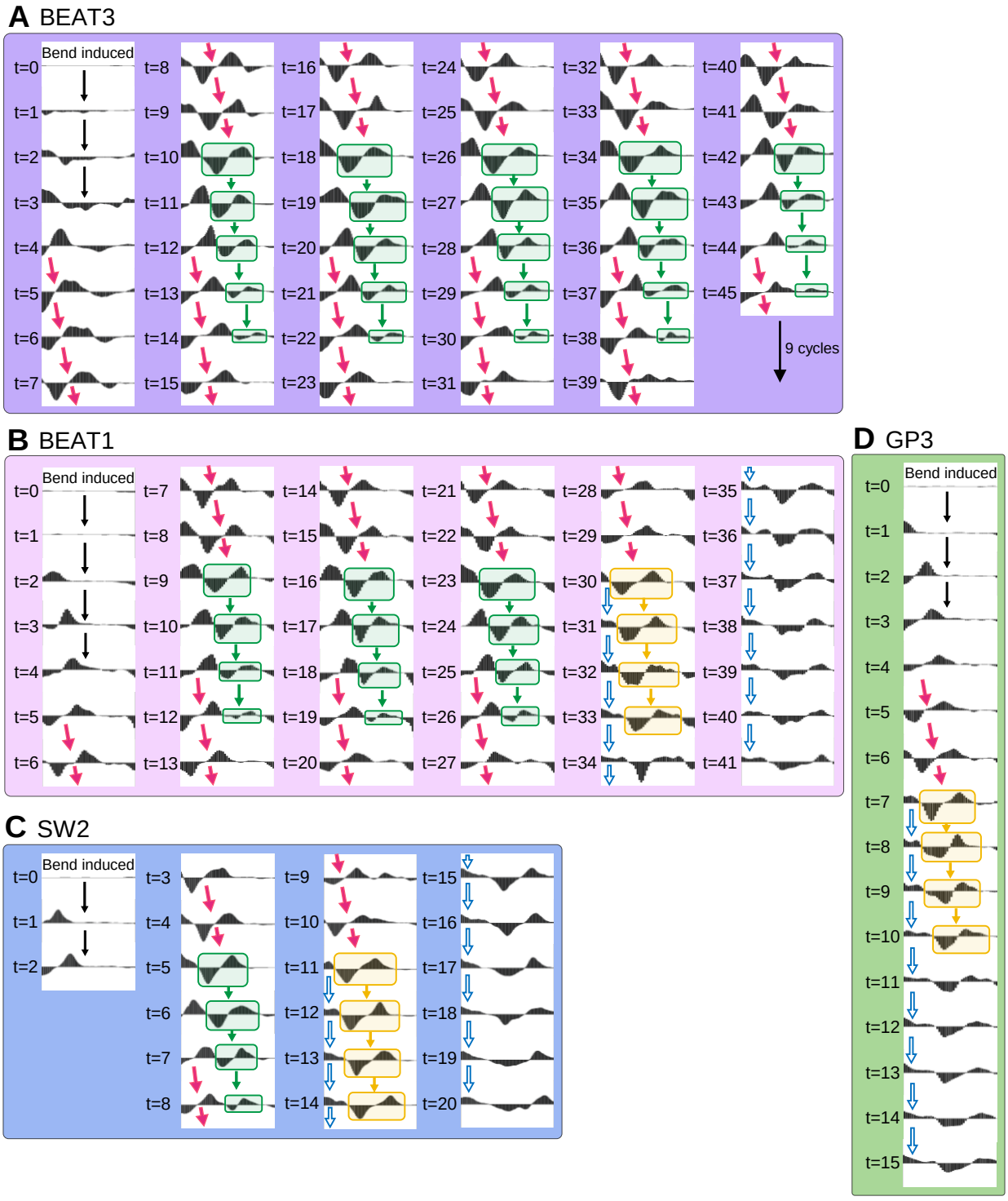
A BEAT3
Bend induced
t=0
t=1
t=2
t=3
t=4
t=5
t=6
t=7
t=8
t=9
t=10
t=11
t=12
t=13
t=14
t=15
t=16
t=17
t=18
t=19
t=20
t=21
t=22
t=23
t=24
t=25
t=26
t=27
t=28
t=29
t=30
t=31
t=32
t=33
t=34
t=35
t=36
t=37
t=38
t=39
t=40
t=41
t=42
t=43
t=44
t=45
9 cycles
B BEAT1
Bend induced
t=0
t=1
t=2
t=3
t=4
t=5
t=6
t=7
t=8
t=9
t=10
t=11
t=12
t=13
t=14
t=15
t=16
t=17
t=18
t=19
t=20
t=21
t=22
t=23
t=24
t=25
t=26
t=27
t=28
t=29
t=30
t=31
t=32
t=33
t=34
t=35
t=36
t=37
t=38
t=39
t=40
t=41
C SW2
Bend induced
t=0
t=1
t=2
t=3
t=4
t=5
t=6
t=7
t=8
t=9
t=10
t=11
t=12
t=13
t=14
t=15
t=16
t=17
t=18
t=19
t=20
D GP3
Bend induced
t=0
t=1
t=2
t=3
t=4
t=5
t=6
t=7
t=8
t=9
t=10
t=11
t=12
t=13
t=14
t=15

Fig. 8.

Time-dependent changes of wave dynamics expressed by the curvature change along flagellar length in BEAT, SW, and GP. BEAT3 (A), BEAT1 (B), and SW2 (C) are the same sperm flagella shown in Fig. 7. The BEAT3 and BEAT1 showed repetitive cyclical oscillation and limited cycle of oscillation (3.5 cycles), respectively. SW2 also showed a limited cycle of oscillation (1.5 cycles). Development of bends on both sides of the flagellum corresponds to the cyclical bending: in BEAT3 (A) mechanically induced bending (started at t=0) appeared as paired bends and grew within 3 s (at t=4-7 s). These paired bends propagated distally (t=8-10 s) and they gradually decreased in size as pairs until t=14 s. The green boxes show the process of bend decay. As changes progress, a more proximal bend grew and developed (t=12-15 s). These processes form the basis of repetitive cyclical oscillation. In contrast, as shown in the examples of limited cycles in BEAT1 (B) and SW2 (C), I did not observe any formation and propagation of paired bends in the proximal region, when the decrease in size of bends did not occur (t=30-33 s in BEAT1; t=11-14 s in SW2). The yellow boxes show the process. Similar responses showing such propagation towards the distal end without a decrease in size of paired bends are also observed in GP3 (D).

References

Baba, S. and Hiramoto, Y. (1978). A quantitative analysis of flagellar movement in echinoderm spermatozoa. *J. Exp. Biol.* **74**, 85-104.

Baba, S. and Mogami, Y. (1985). An approach to digital image analysis of bending shapes of eukaryotic flagella and cilia. *Cell Motil.* **5**, 475-489.

Bayly, P. V. and Dutcher, S. K. (2016). Steady dynein forces induce flutter instability and propagating waves in mathematical models of flagella. *J. R. Soc.* **13**, 20160523.

Boryshpolets, S., Cosson, J., Bondarenko, V., Gillies, E., Rodina, M., Dzyuba, B. and Linhart, O. (2013). Different swimming behaviors of sterlet (*Acipenser ruthenus*) spermatozoa close to solid and free surfaces. *Theriogenelogy.* **79**, 81-86.

Brokaw, C. J. (1972). Computer simulation of flagellar movement: Ⅰ. Demonstration of stable bend propagation and bend initiation by the sliding filament model. *Biophys. J.* **12**, 564-586.

Brokaw, C. J. (1975). Effects of viscosity and ATP concentration on the movement of reactivated sea-urchin sperm flagella. *J. Exp. Biol.* **62**, 701-719.

Brokaw, C. J. (1976). Computer simulation of flagellar movement: Ⅳ. Properties of an oscillatory two-state cross-bridge model. *Biophys. J.* **16**, 1029-1041.

Brokaw, C. J. (1982). Models for oscillation and bend propagation by flagella. *Symp. Soc. Exp. Biol*. **35**, 313-38.

Brokaw, C. J. (1985). Computer simulation of flagellar movement: Ⅵ. Simple curvature-controlled models are incompletely specified. *Biophys. J.* **48**, 633-642.

Brokaw, C. J. (1989). Direct measurements of sliding between outer doublet microtubules in swimming sperm flagella. *Science* **243,** 1594-1596.

Brokaw, C. J. (1991). Microtubule sliding in swimming sperm flagella: direct and indirect measurements on sea urchin and tunicate spermatozoa. *J. Cell Biol*. **114**, 1201-1215.

Brokaw, C. J. (2002). Computer simulation of flagellar movement: Ⅷ. Coordination of dynein by local curvature control can generate helical bending waves. *Cell Motil. Cytoskeleton*. **53**, 103-124.

Brokaw, C. J. (2005). Computer simulation of flagellar movement: Ⅸ. Oscillation and symmetry breaking in a model for short flagellar and nodal cilia. *Cell Motil. Cytoskeleton*. **60**, 35-47.

Camalet, S. and Julicher, F. (2000). Generic aspects of axonemal beating. *New J. Phys.* **24**, 1-23.

Cosson, J., Huitorel, P. and Gagnon, C. (2003). How spermatozoa come to be confined

to surfaces. *Cell Motil. Cytoskeleton*. **54**, 56-63.

Eshel, D., Shingyoji, C., Yoshimura, K., Gibbons, I. R. and Takahashi, K. (1991). Evidence for an inequality in the forces that generate principal and reverse bends in sperm flagella. *J. Cell Sci*. **100**, 213-218.

Eshel, D., Shingyoji, C., Yoshimura, K., Gibbons, I. R. and Takahashi, K. (1992). The phase of sperm flagellar beating is not conserved over a brief imposed interruption. *Exp. Cell Res.* 202, 552-555.

Gibbons, I. R. (1981). Transient flagellar waveforms during intermittent swimming in sea urchin sperm: Ⅱ. Analysis of tubule sliding. *J. Muscle Res. Cell Motil*. **2**, 83-130.

Gibbons, B. H. and Gibbons, I. R. (1972). Flagellar movement and adenosine triphosphatase activity in sea urchin sperm extracted with Triton X-100. *J. Cell Biol.* **54**, 75-97.

Gibbons, B. H. and Gibbons, I. R. (1980). Transient flagellar waveforms during intermittent swimming in sea urchin sperm: Ⅰ. Wave parameters. *J. Muscle Res. Cell Motil*. **1**, 31-59.

Gibbons, I. R., Shingyoji, C., Murakami, A. and Takahashi, K. (1987). Spontaneous recovery after experimental manipulation of the plane of beat in sperm flagella. *Nature*, **325**, 351-352.

Hayashi, S. and Shingyoji, C. (2008). Mechanism of flagellar oscillation‐bending-induced switching of dynein activity in elastase-treated axonemes of sea urchin sperm. *J. Cell Sci*. **121**, 2833-2843.

Hayashibe, K., Shingyoji, C. and Kamiya, R. (1997). Induction of temporary beating in paralyzed flagella of *Chlamydomonas* mutants by application of external force. *Cell Motil. Cytoskeleton* **37**, 232-239.

Ishikawa, R. and Shingyoji, C. (2007). Induction of beating by imposed bending or mechanical pulse in demembranated, motionless sea urchin sperm flagella at very low ATP concentrations. *Cell Struct. Funct.* **32.** 17-27.

Izawa, Y. and Shingyoji, C. (2020). Mechanical induction of oscillatory movement in demembranated, immotile flagella of sea urchin sperm at very low ATP concentrations. *J. Exp. Biol.* **223.** doi:10.1242/jeb. 225797

Lin, J. and Nicastro, D. (2018). Asymmetric distribution and spatial switching of dynein activity generates ciliary motility. *Science*. **360**, PMID: 29700238.

Lindemann, C. B. and Rikmenspoel, R. (1972). Sperm flagella: autonomous oscillations of the contractile system. *Science* **175,** 337-338.

Lindemann, C. B. (1994a). A “geometric clutch” hypothesis to explain oscillations of the axoneme of cilia and flagella. *J. Theor. Biol.* **168**, 175-189.

Lindemann, C. B. (1994b). A model of flagellar and ciliary functioning which uses the forces transverse to the axoneme as the regulator of dynein activation. *Cell Motil. Cytoskeleton*. **29**, 141-154.

Morita, Y. and Shingyoji, C. (2004). Effects of imposed bending on microtubule sliding in sperm flagella. *Curr. Biol.* **14**. 2113-2118

Murase, M. (1991).Excitable dynein model with multiple active sites for large-amplitude oscillations and bend propagation in flagella. *J. Theor. Biol*. **149**, 181-202.

Oda, T., Yanagisawa, H., Yagi, T. and Kikkawa, M. (2014). Mechanosignaling between central apparatus and radial spokes controls axonemal dynein activity. *J. Cell Biol.* **204**, 807-819.

Okuno, M. and Hiramoto, Y. (1976). Mechanical stimulation of starfish sperm flagella. *J. Exp. Biol.* **65**, 401-413.

Prokopchuk, G., Dzyuba, B., Bondarenko, O., Rodina, M. and Cosson, J. (2015). Motility initiation of sterlet sturgeon (*Acipenser ruthenus*) spermatozoa: Describing the propagation of the first flagellar waves. *Theriogenelogy.* **84**, 51-61.

Satir, P. (1968). Studies on cilia Ⅲ. Further studies on the cilium tip and a 'sliding filament' model of ciliary motility. *J. Cell Sci*. **39**, 77-94.

Shingyoji, C. (2018). Regulation of dynein-driven ciliary and flagellar movement. In *Dyneins: Structure, Biology and Disease*, 2nd edn, pp. 336-367. London, UK: Elsevier Inc.

Shingyoji, C., Katada, J., Takahashi, K. and Gibbons, I. R. (1991a). Rotating the plane of imposed vibration can rotate the plane of flagellar beating in sea-urchin sperm without twisting the axoneme. *J. Cell Sci*. **98**, 175-181.

Shingyoji, C., Murakami, A. and Takahashi, K. (1977). Local reactivation of Triton-extracted flagella by iontophoretic application of ATP. *Nature* **265**, 269-270.

Shingyoji, C., Gibbons, I. R., Murakami, A. and Takahashi, K. (1991b). Effect of imposed head vibration on the stability and waveform of flagellar beating in sea urchin spermatozoa. *J. Exp. Biol*. **156,** 63-80.

Shingyoji, C., Nakano, I., Inoue, Y. and Higuchi, H. (2015). Dynein arms are strain-dependent direction-switching force generators. *Cytoskeleton.* **72**, 388-401.

Shingyoji, C., Yoshimura, K., Eshel, D., Takahashi, K. and Gibbons, I. R. (1995). Effect of beat frequency on the velocity of microtubule sliding in reactivated sea urchin sperm flagella under imposed head vibration. *J. Exp. Biol.* **198,** 645-653.

Summers, K. E. and Gibbons, I. R. (1971). Adenosine triphosphate-induced sliding of tubules in trypsin-treated flagella of sea-urchin sperm. *Proc. Natl. Acad. Sci. USA* **68,** 3092-3096.

Warner, F. D. and Satir, P. (1974). The structural basis of ciliary bend formation. Radial spoke positional changes accompanying microtubule sliding. *J. Cell Biol*. **63**, 35-63.
Yoke, H. and Shingyoji, C. (2017). Effects of external strain on the regulation of microtubule sliding induced by outer arm dynein of sea urchin sperm flagella. *J. Exp. Biol.* **220,** 1122-1134.